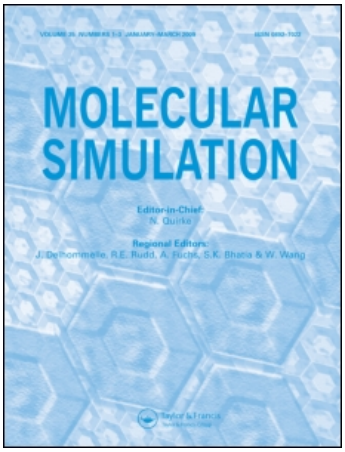

Molecular Simulation
Publication details, including instructions for authors and subscription information:
http://www.informaworld.com/smpp/title~content=t713644482

Molecular Dynamics Glass Simulation and Equilibration Techniques

S. Gruenhut[a]; M. Amini[ab]; D. R. Macfarlane[a]; P. Meakin[a]
[a] Department of Chemistry, Monash University, Melbourne, Australia [b] Department of Physics, Isfahan University of Technology, Isfahan, Iran

To cite this Article Gruenhut, S. , Amini, M. , Macfarlane, D. R. and Meakin, P.(1997) 'Molecular Dynamics Glass Simulation and Equilibration Techniques', Molecular Simulation, 19: 3, 139 — 160
To link to this Article: DOI: 10.1080/08927029708024147
URL: http://dx.doi.org/10.1080/08927029708024147

Molecular Simulation, 1997, Vol. 19, pp. 139–160
Reprints available directly from the publisher
Photocopying permitted by license only

MOLECULAR DYNAMICS GLASS SIMULATION AND EQUILIBRATION TECHNIQUES

S. GRUENHUT, M. AMINI*, D. R. MACFARLANE and P. MEAKIN

Department of Chemistry, Monash University, Clayton, Melbourne, 3168, Australia

(Received October 1996; Accepted January 1997)

To determine the effect of molecular dynamics simulation methodology on both the structural and dynamic properties of fluoride glasses, a large number of simulations were carried out using the same simulation box, potential, initial starting point and final temperature. It has been shown that the simulation methodology is, at least, as important as the potential in determining the final glass structure. Two useful tools have been developed which can, with more accuracy than present techniques, determine the point of homogeneity or equilibrium in glass simulations. These are a spherical average of all ions and a spherical average of each ion type within a sphere of radius half a box length. It has also been shown that, for a constant volume simulation, the use of the canonical ensemble (NVT) can lead to a structure that is not in its minimum potential energy configuration. Therefore, a combination of the canonical (NVT) and microcanonical (NVE) ensembles were used. Finally, a methodology is suggested that appears optimal for molecular dynamics glass simulations of the type performed in this paper.

Keywords: Molecular dynamics; simulation and equilibration techniques; computer simulation methodology; structural analysis; fluoride glasses; ZBN

INTRODUCTION

Fluoride glasses are technologically superior to silica for some applications in the communications industry. For instance, fluoride glasses have theoretically lower attenuation at their optimum wavelength, a 100 times less, than silica and thus have a potential to be used as low loss optical fibres, p28 [1]. When doped with certain rare earths, fluoride fibres can produce

*On sabbatical from Department of Physics, Isfahan University of Technology, Isfahan, Iran.

higher efficiency active devices, such as fibre amplifiers and lasers, p4 [1]. The potential to make low loss fibres from fluoride glass has not been realised as experimentalists have, to date, been unable to make a glass which approaches the calculated theoretical attenuation. As the physical properties of the glass are related to the structure, the full potential of fluoride fibres will only be realised by determining the structure in a detailed, atomistic way and understanding the effect of structure on the physical properties. Fluoride glasses are amorphous solids and hence it is impossible experimentally to uniquely determine the three dimensional structure [2]. However, the combination of modelling and molecular dynamics is a powerful technique that, when used correctly, enables the study of the three dimensional glass structure as well as the interaction of all the ions in the glass.

In the past, molecular dynamics has been used to model the Zr/Ba binary fluoride glass system as well as other systems. However, these simulations resulted in unrealistic physical properties, for example high pressures, incorrect density or incorrect structure [3–8]. These problems are caused either by the incorrect choice of potential and its parameters or the simulation methodology. Simulation methodology encompasses the type of ensemble, number of particles, time step, equilibration temperature and time, quench rate, data collection. A literature search of molecular dynamics in the fluoride glass area has shown that most studies have tried to address the selection and tuning of the potential [4,9–13]. However, the simulation methodology has only partially been investigated. For instance Brawer and Weber [14] have suggested a criterion for reaching equilibration, which is that the statistical averages of the system (total energy, potential energy, pressure, temperature, etc.) should not change when the period of the simulation is increased substantially. This period cannot be determined precisely as numerical and computational errors cause drifts in the statistical averages, p96 [15], [16]. The simulated structure will also reflect these energy drifts and cannot be used to determine equilibration. An additional criteria suggested is that the particles should show sufficient diffusion, p171 [14], [17]. The subject of drift in total energy, effects of sample size and time step have been discussed by many authors (for example [15–18]); however the choice of equilibration temperature, equilibration time, quench rate and ensemble used for constant temperature simulations and data collection have not. The effect of the methodology on the structure and other results has also not been investigated [4,9–13]. This paper will describe the computer techniques necessary to ensure a well equilibrated glass simulation is performed. Trade-offs in quench rate will be illustrated, along with a new

criteria that can be used to ensure an equilibrated initial structure. Structural differences in the final glass as a result of different methodologies will also be shown.

COMPUTATIONAL

In order to determine the most suitable molecular dynamics methodology, many glasses were simulated using different equilibration periods, quench rates and data collection methods. The Buckingham pair potential was used for all of these simulations in the form (ignoring the van der Waals terms [4,19]):

$$U_{ij} = \frac{-q_i q_j}{4\pi\varepsilon_0 r_{ij}} + A_{ij}\exp\left[\frac{-r_{ij}}{\rho_{ij}}\right] \tag{1}$$

where q_i and q_j are the charges of the individual ions, r_{ij} is the distance between the ions, A_{ij} is the depth of the potential well and ρ_{ij} is the slope of the short range exponential repulsion [20]. Potential tuning was initially performed by selecting a suitable X-ray structure of a $BaNaZr_2F_{11}$ crystal [21]. The crystal structure was then convolved with the Gaussian distributions, defined by the anisotropic temperature factors, to produce a radial distribution function (RDF) for the crystal at room temperature [22]. The initial Buckingham potential parameters were selected for the crystal using the method of Lucas *et al.* [4] with ρ_{ij} being fixed at 0.29 Å to simplify tuning. The value of A_{ij} for each pair potential was then fine tuned by simulating the crystal structure at 500 K and comparing the simulated RDFs against those from X-ray diffraction. When no appreciable crystal structure improvement could be made, the potential parameters were accepted, see Table I.

All the simulations were performed using the molecular dynamics program FUNGUS [23,24], supplied by BIOSYM/MSI, with the same initial atomic coordinates. The ZBN glass (57 mole% ZrF_4: 21.5 mole% BaF_2: 21.5 mole% NaF) was simulated with a box length of 22.227 Å and periodic boundary conditions were imposed. The number of ions in the system was 785 (114 Zr, 43 Ba, 43 Na and 585 F). To avoid imposing any initial structure on the system, all ions of the same type were placed adjacent to each other. The initial coordinates of the system corresponded to a NaCl structure of similar box size. A time step of 1 fs was chosen to ensure that there was greater than 15–33 time steps (70) per molecular vibrational

TABLE I Potential Parameters for all simulations of Zr/Ba/Na Glass

Pair Function	A_{ij} (*eV*)
Ba–Ba	100000
Ba–Na	100000
Ba–F	3500.8
Ba–Zr	35000
Na–Na	5000
Na–F	600
Na–Zr	117.6
F–F	1000
F–Zr	1800
Zr–Zr	77.8

period p474 [15]. Using this time step there was no drift in energy, the change in the ratio of total energy (TE) to kinetic energy (KE) (ΔTE/KE) being less than 0.001% over 100 ps.

The glass simulations have been subdivided according to the simulation procedure and are listed Table II. Glass A1 has an initial temperature of 6000 K with an equilibrium period consisting of 3 ps NVT (number of atoms, simulation box volume and temperature are held constant) followed by 97 ps NVE (number of atoms, simulation box volume and total energy are held constant). The melt was then quenched in a step wise fashion with a temperature decrement of 500 K using 3 ps NVT followed by an equilibration simulation of 17 ps NVE. At 300 K, a 3 ps NVT and 17 ps NVE simulation was performed. Glass A2 is the same as glass A1 with the exception of the high temperature initial equilibration period being 7 ps NVE and the quench step NVE period being 7 ps. Class B glasses were produced in a similar fashion to class A but only used the NVT ensemble. Glass C consists of a 6000 K 10 ps NVT equilibration simulation followed by an immediate quench from 6000 K to 300 K. Class D glasses differ from class B glasses only in the initial temperatures and quench rates. The whole simulation for glass E was carried out at 300 K.

The thermodynamic and structural results were output every 20 time steps during the simulation. In order to remove the effect of the natural fluctuations of the system, the thermodynamic data was averaged over 7 ps with both average and standard deviation data being obtained. The coordinate file was further analysed by an in-house program to produce coordination, nearest neighbour angle and bridging information. The coordination number distributions (CNDs) where calculated for each pair of ions, *i-j*, by using each ion of type *i* (Zr, Ba, Na, F) as the centre of a sphere up to a

TABLE II Characteritics of the twelve different simulations

Glass	*Initial*	*Quench*					*300 K Simulation*	*Total Simulation*	*Quench Rate*
	Temperature (K)	*Equilibration Method*	*Equilibration period (ps)*	*Temperature Decrement (K)*	*Ensemble*	*Duration (ps)*	*Period (ps)*	*Time (ps)*	10^{12} *K/s*
A1	6000	NVT/NVE	3/97	500	NVT/NVE	3/17	20	340	24.8
A2	6000	NVT/NVE	3/7	500	NVT/NVE	3/7	20	140	51.8
B1	6000	NVT	20	500	NVT	10	20	150	51.8
B2	10000	NVT	10	500	NVT	10	20	220	51.1
B3	6000	NVT	10	500	NVT	10	20	140	51.8
C	6000	NVT	10	–	–	–	10	20	Immediate
D1	4500	NVT	10	100	NVT	0.5	10.5	42.5	187
D2	3500	NVT	10	100	NVT	0.5	10.5	36.5	193
D3	2500	NVT	10	100	NVT	0.5	10.5	31.5	191
D4	1500	NVT	10	100	NVT	0.5	10.5	26.5	185
D5	500	NVT	10	100	NVT	0.5	10.5	21.5	133
E	300	NVT	–	0	NVT	–	23	20	–
F	500–6000	NVT	10	–	–	–	–	10	–

cutoff radius and counting the number of atoms of type j (Zr, Ba, Na, F) within this sphere. The cutoff radius chosen is the position of the first minimum of the RDFs, see Table III.

An additional tool used for equilibration analysis was the spherical average of the number ions of type j around type i within a radius r, $n_{ij}(r)$. These averages were computed over a period of 7 ps using [17, 25]:

$$n_{ij}(r) = \int_0^r \rho_j g_{ij}(r) 4\pi r^2 \, dr \tag{2}$$

where ρ_j is the density of the ions being examined and $g_{ij}(r)$ is the radial distribution function of atom of type j about atom type i. The spherical average of a single ion type, using a radius equal to half the simulation box length L, is denoted by n_j. Similarly, the spherical average of all ions in the system, computed from the addition of the n_j values for Ba–Ba, F–F, Na–Na and Zr–Zr, is denoted by n_{all}. The expected value of n_j for a homogeneous distribution, n_j^*, is a fraction of the total number of ions of type j within the simulation box, N_j, minus the centre atom:

$$n_j^* = \frac{\pi N_j}{6} - 1 \tag{3}$$

The expected value of n_{all} for a homogeneous distribution, n_{all}^*, can also be computed by summing the individual n_j^* values for each ion type.

TABLE III RDF peak positions (average nearest neighbour distances) and average coordination numbers for the simulated ZBN glass A1 as well as the cutoff radii used for all glasses. Experimental results for various compositions of Zr/Ba binary glasses from references [26–32] are also shown

Ion Pair	*RDF peak (Å)*		*Average CN*		*Cutoff Radius*
	Simulation (± 0.05)	*Experiment*	*Simulation* (± 0.03)	*Experiment*	*(Å)*
Ba–Ba	4.09/4.50	4.03–4.16	2.24		5.00
Ba–Na	4.17		2.15		5.50
Ba–F	2.63	2.6–2.8	6.84		3.00
Ba–Zr	4.33	4.03–4.16	6.94		5.00
Na–Na	3.37		2.13		4.60
Na–F	2.19		5.86		3.00
Na–Zr	3.82		5.76		4.70
F–F	2.56		7.93		3.30
Zr–F	1.97	2.06–2.7	7.26	6.0–8.0	2.80
Zr–Zr	4.07	4.03–4.16	4.14		4.55

To demonstrate how different values of n_j may be obtained, consider placing N atoms into a spherical volume whose radius is much less than half the length of the simulation box. When the spherical average is computed all the atoms become the centre for a sphere of radius L. All these spheres will contain $N-1$ atoms and hence $n_j > n_j^*$. If, on the other hand, only two ions are placed in close proximity to each other in the simulation box, forming a cluster, with the rest being distributed homogeneously, only those spheres containing this cluster will have $n_j > n_j^*$. The majority of spheres will consequently have $n_j < n_j^*$ and hence, the simulation box will have $n_j < n_j^*$. Therefore, although under certain conditions of clustering both $n_j > n_j^*$ and $n_j < n_j^*$ are possible, a fully equilibrated glass is expected to have values which are close to those for a homogeneous distribution.

RESULTS

The variation of potential energy (PE) with temperature, averaged over 7 ps, of glass A1 is displayed in Figure 1. The standard deviation of the potential energy, less than 0.05%, is contained within the size of the symbols. The PE

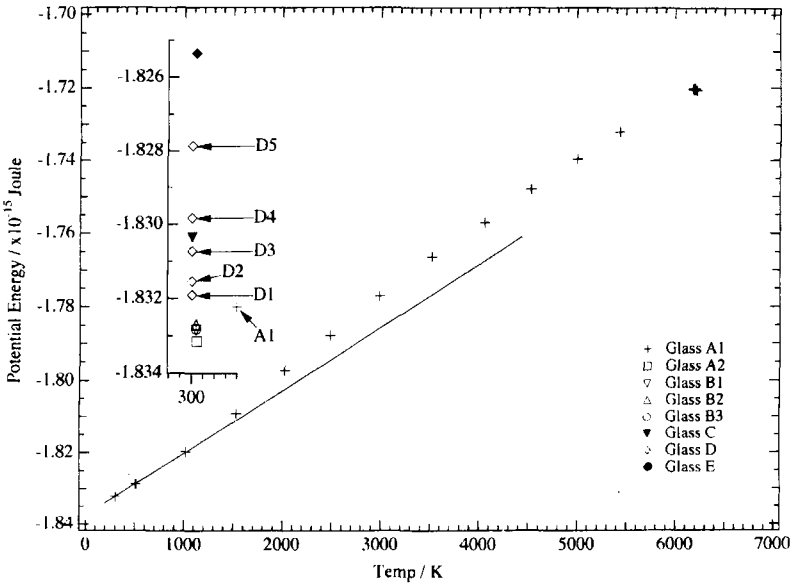

FIGURE 1 Variation of potential energy, averaged over 7 ps, for glass A1. The standard deviation of potential energy is contained within the size of the symbols and is therefore not shown. The inset graph indicates the potential energy for all glasses at 300 K.

curve has a broad slope change close to 2000 K probably indicating a broad "glass" transition. The PEs of the other glasses follow the trend of glass A1 and are therefore not shown. The inset graph shows the potential energy obtained from the 300 K simulations for all glasses. For most glasses the PE decreases in proceeding from class E to class A. The exceptions are glass C which lies amongst class D and glass A1 which lies just below glass D1.

The final values of mean squared displacement (MSD), after 7 ps, for glass A1 are shown in Figure 2. The data of glass A1 is again representative of the other glasses which are therefore not shown. A glass transition is indicated by a broad change in gradient of the final MSD curve at approximately 2000 K. The inset graph, 2A, indicates the final MSD values for the glasses at 300 K. According to these results, the glasses can be categorised into two groups: glass C and the rest, with glass C having the largest final MSD value. Inset graph 2B shows the evolution with time of the final values of MSD during the high temperature, 6000 K, equilibration period for glass A1.

The spherical average, n_{all}, for all of the glasses are displayed in Figure 3. The corresponding expected value for a homogeneous system, n^*_{all}, is also shown. The inset graph shows the values of n_{all} and n^*_{all} versus time during

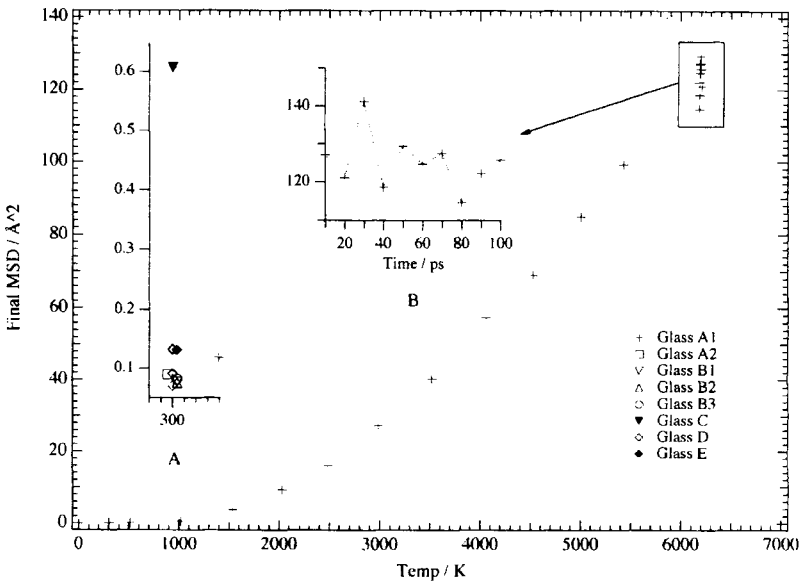

FIGURE 2 Final mean squared displacement (MSD) versus temperature for glass A1. Final MSD values for all glasses at 300 K are shown in inset graph 2A. Evolution of MSD during equilibration at 6000 K for glass A1 is displayed in inset graph 2B.

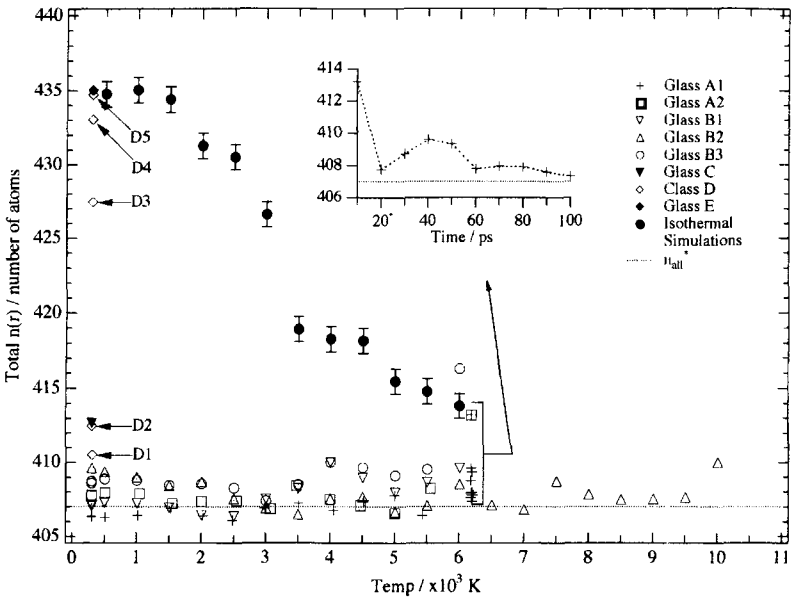

FIGURE 3 Spherical average of all ions using a sphere of radius half a simulation box length, n_{all}, versus temperature for all glasses. The value of n_{all} for a set of isothermal simulations using the same starting configuration and n_{all} for a homogeneous system n^*_{all} are also shown. The inset graph displays the n_{all} and n^*_{all} during equilibration at 6000 K. All data displayed are determined over 7 ps. The standard deviation, which represents the fluctuations in n_{all}, is indicated for clarity only on the isothermal simulations.

the equilibration of glass A1. To determine the effect of the initial configuration and equilibration temperature on the final structure, a set of isothermal simulations were also performed. These consisted of 10 ps NVT at a single temperature between 500 and 6000 K using the same initial coordinates. For clarity, the magnitude of the fluctuations in n_{all} are only indicated for these simulations. Not only do the isothermal simulations have n_{all} values which are higher than for a homogeneous distribution, n^*_{all}, but they increase with decreasing temperature with an abrupt increase occurring between 3000 K and 2500 K. During equilibration, glass A1 has a progressive decrease in the value of n_{all} towards n^*_{all}. Both class A and B glasses, once equilibrated, have a consistent value of n_{all} across their temperature range with glass A1 having the least variation. Examining glass B2 below 1500 K, the value of n_{all} diverges from n^*_{all}.

The spherical average, n_j, for each glass and ion type was calculated and analysed at each temperature. Concentrating on 300 K, Figure 4 shows these results as a histogram of the ratio n_j/n^*_j for the glasses A1, B1, C and E.

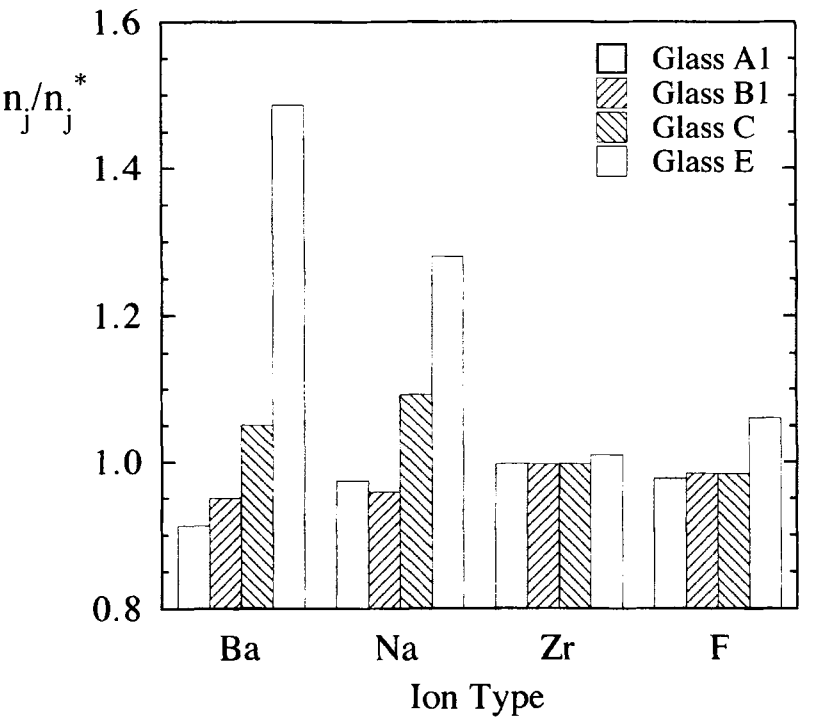

FIGURE 4 The ratio of the spherical average of a particular ion type using a sphere of radius half a simulation box length, n_j, to the value for a homogeneous distribution, n_j^*, for glasses A1, B1, C and E at 300 K. The value of n_j was averaged over 7ps.

The value for a homogeneous distribution, n_j^*, is therefore one. Moving from glass E to glass A1 there is a steady decrease of n_j towards n_j^*. However, the rate of decrease is not the same for all ion types. In glasses, C, B1 and A1, both the fluoride and zirconium ions have a n_j value close to n_j^*. However, barium and sodium only attain a value of n_j close to n_j^* in glasses B1 and A1.

The RDFs for all combinations of atoms of glass A1 at 300 K are shown in Figure 5. These are calculated up to half a box length, but are only indicated up to 6 Å for clarity. The sharpest and most well defined $g(r)$ peaks are for Zr–Zr and Zr–F, indicating that they have the most structure. The position of the first RDF peak (average nearest neighbour distance) and average coordination number are indicated in Table III. The cutoff, i.e. the position of the first RDF pair minima, which was used for determining the NNADs, CNs and CNDs for all glasses is also displayed. The experimentally determined RDF peak positions and average CNs are listed for various compositions of Zr/Ba binary fluoride glass [26–32]. These values

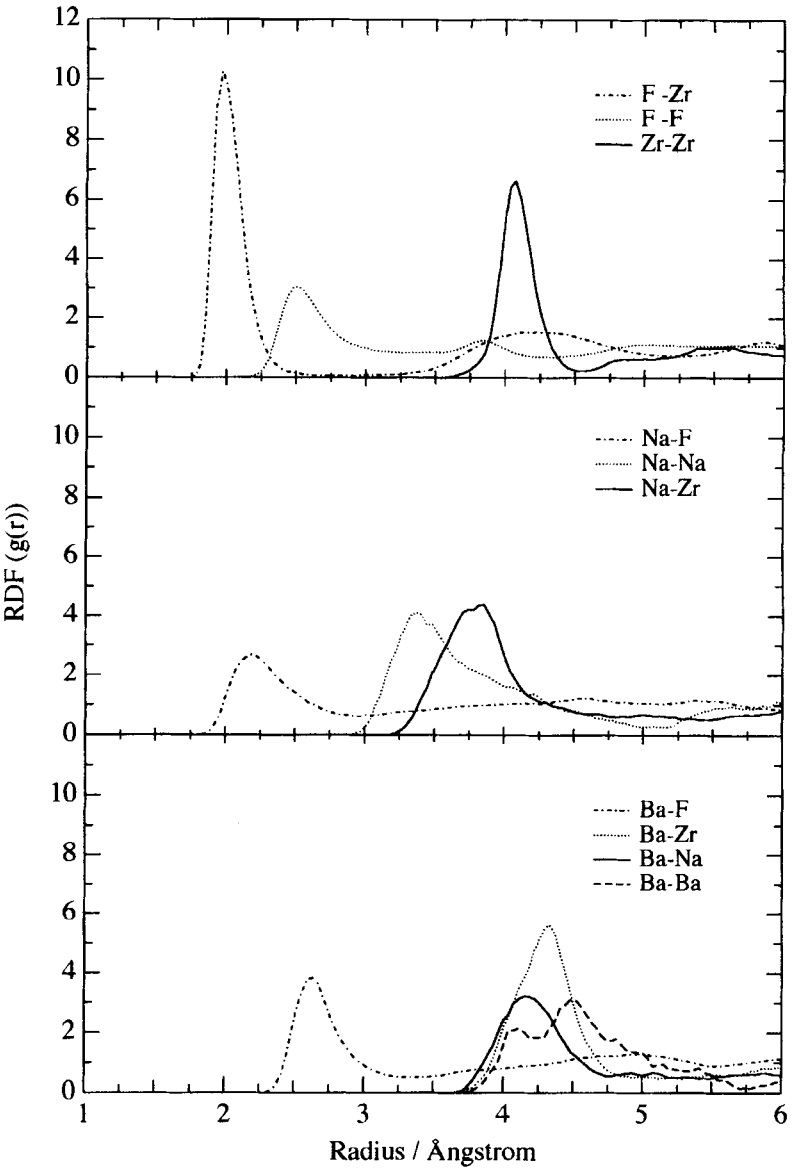

FIGURE 5 Radial distribution functions, RDFs, for all ion pair interactions of Zr/Ba/Na glass A1 averaged over at 300 K.

are in general agreement with glass A1. For example, the position of glass A1's first RDF peaks for Zr–F, Zr–Zr and Ba–Ba are, 1.97, 4.07 and 4.09 Å with the respective experimental values being between 2.06–2.7, 4.03–4.16

and 4.03–4.16 Å. The errors shown for the RDF peak positions and average coordination numbers are based upon measurement accuracy. These errors are different for each ion type and reflect the sharpness of the RDF peak as well as the definition of the first RDF minima.

The radial distribution functions for glasses A1, B1, C and E are compared in Figure 6. Generally, the $g(r)$ peak heights decrease in moving from glass E to glass A1. The exception is Zr–F which has no trends evident. Glasses A1, B1 and C have Zr–Zr and Na–Na $g(r)$ peaks which are closely grouped and significantly lower than that for glass E. This trend is also followed for Ba–Ba, with glasses A1, B1 and C having $g(r)$ peaks significantly lower than that for glass E. However in this case glass A1 has a Ba–Ba $g(r)$ peak which is significantly lower than either glass B1 or C. Overall, the Ba–Ba radial distribution functions show the most variation in peak height, while the Zr–F radial distribution functions show the least variation.

A comparison of selected nearest neighbour angle distributions (NNAD), F–Zr–F, Zr–Zr–Zr, Na–Na–Na and Ba–Ba–Ba and CNDs (Zr–F, Zr–Zr, Na–Na, and Ba–Ba) for glasses A1, B1, C and E, are displayed in Figures 7 to 10. Since there is no direct height correlation all the NNADs and CNDs have been scaled such that their maximum peak height is one. Generally, the higher the coordination number, the lower the nearest neighbour angle. The Ba–Ba–Ba and Na–Na–Na NNADs for glasses A1 to E show some similarity in the peak positions while there are none in the CNDs. However, the NNADs for Zr–Zr–Zr and F–Zr–F show a far greater similarity but as previously, with no similarities evident in the CNDs.

The average coordination numbers (CN) for selected ion pairs of all the glasses at 300 K are indicated in Table IV. The average CNs for Zr–F, Ba–F, Na–F are very similar. However, the average CNs of Zr–Zr, Ba–Ba and Na–Na increase dramatically for glasses D3 to D5 and glass E. The greatest increase in average CN is observed for Ba–Ba and the least for Zr–Zr.

DISCUSSION

To determine the effect of simulation methodology on both the structural and dynamic properties, a large number of simulations have been carried out in this study, all using the same simulation box, potential, initial starting point and final temperature. The twelve different glass simulations, subdivided into 5 different classes, are outlined in Table II and demonstrate the effect of ensemble, equilibration temperature, equilibration period and quench rate on the simulations.

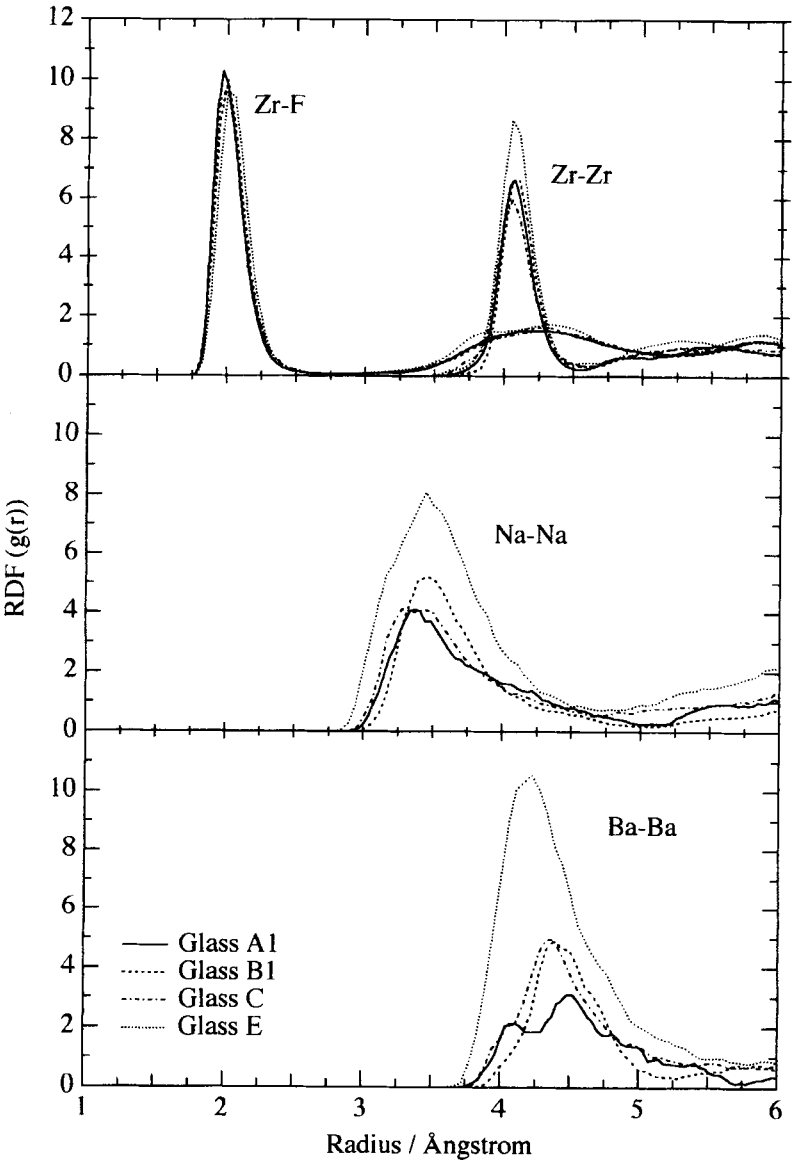

FIGURE 6 Selected radial distribution functions for glasses, A1, B1, C and E at 300 K are compared.

Glass A1 has values of nearest neighbour distances and coordination numbers that are closest to those experimentally obtained for various Zr/Ba glasses [26–32]. The close agreement of the Ba–Ba nearest neighbour

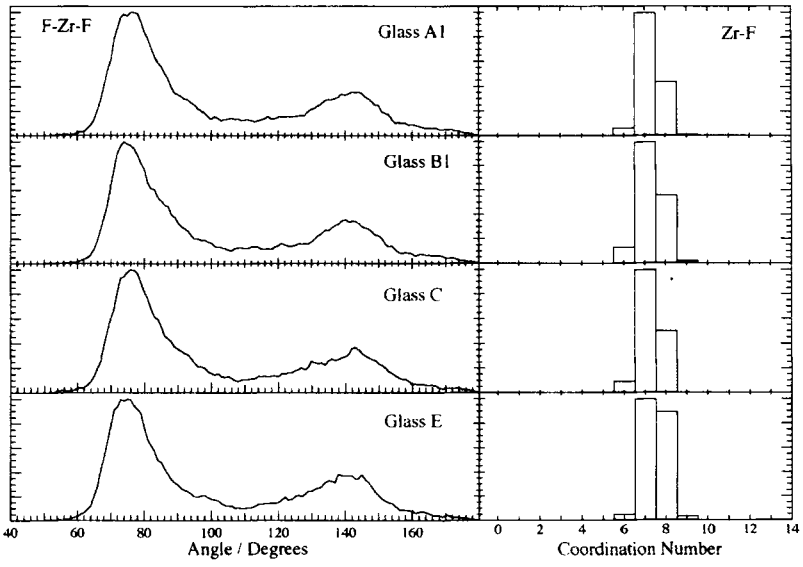

FIGURE 7 A comparison of F–Zr–F nearest neighbour (bond) angle distributions, NNADs, and Zr–F coordination number distribution, CND, for glasses A1, B1, C and E at 300 K.

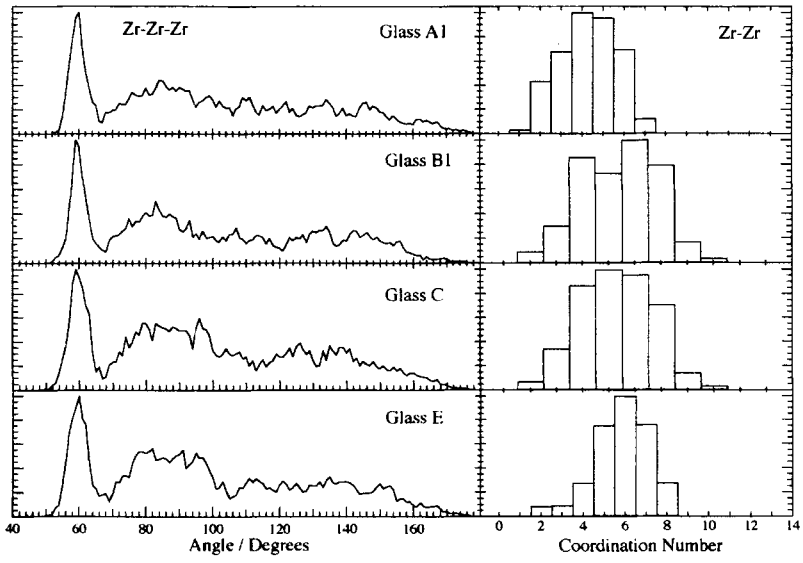

FIGURE 8 The Zr–Zr–Zr nearest neighbour angle distributions and Zr–Zr coordination number distributions for glasses A1, B1, C and E at 300 K are compared.

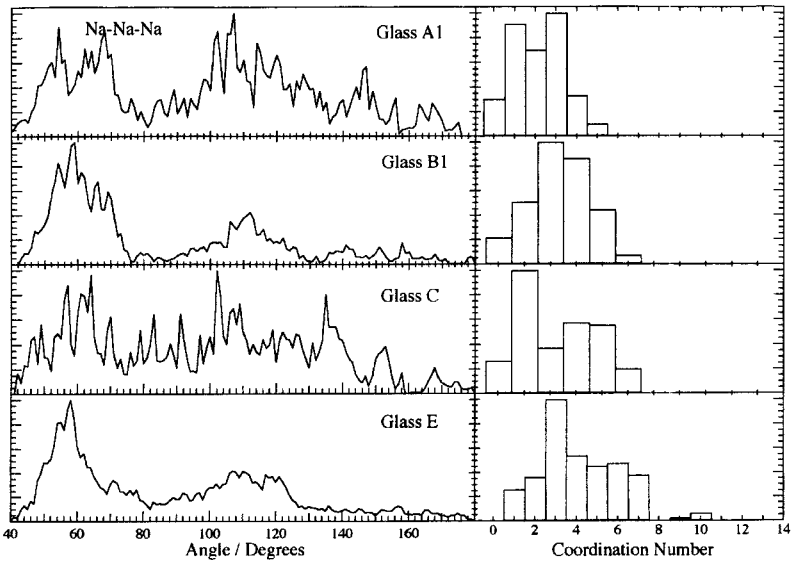

FIGURE 9 Na–Na–Na nearest neighbour anlge distributions and Na–Na coordination number distributions for glasses A1, B, C and E at 300 K.

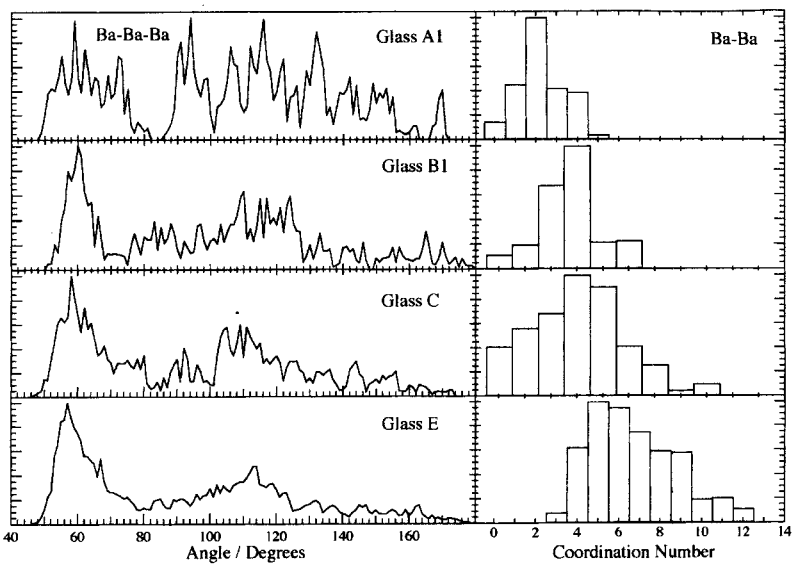

FIGURE 10 Glasses A1, B1, C and E Ba–Ba–Ba nearest neighbour angle distributions and Ba–Ba coordination number distribution at 300 K.

TABLE IV Average coordination number for selected coordination number distributions

Glass	*Ba–F*	*Na–F*	*Zr–F*	*Ba–Ba*	*Na–Na*	*Zr–Zr*
A1	6.8	5.9	7.3	2.2	2.1	4.3
A2	6.8	6.0	7.2	2.4	2.4	4.2
B2	6.7	5.8	7.3	2.4	2.2	4.3
B1	6.9	5.7	7.3	2.7	2.3	4.4
B3	6.8	5.9	7.2	2.3	2.4	4.2
C	6.7	5.8	7.3	3.0	2.3	4.3
D1	6.8	5.9	7.2	2.8	2.0	4.2
D2	6.6	6.0	7.3	2.5	2.2	4.3
D3	6.8	5.7	7.4	5.8	3.3	5.1
D4	6.7	5.5	7.5	6.6	3.9	5.5
D5	6.7	5.6	7.6	6.8	4.5	5.8
E	6.6	5.6	7.5	6.7	4.1	5.8

distance with the experimental values has particular significance as barium is one of the slowest diffusing ions and therefore a good indicator for equilibrium. The other slow moving ion, Zr, was not effected due to its higher charge. A comparison of the Ba–Ba and Ba–Na RDFs for glass A1 against those of glass A2 and classes B and C confirm this. Both these RDF peaks show a greater structural definition in glass A1 than in the other glasses. Glass A1 also has the least variation in n_{all}, with all values, after equilibration, being close to that for a homogeneous distribution. The increase in the equilibration period and the reduction in the quench rate for glass A1 decreases the possibility of locking in high energy liquid structures and improves the homogeneity of the final structure simulated. Hence, greater correlation with experimental and theoretical values are obtained.

Before a suitable equilibration methodology, ensemble(s), temperature and period can be determined, one or more criteria were first established to determine the point at which both a equilibrated and homogeneous simulation was reached. Two criteria frequently used are; (i) a constant minimum value of potential energy and; (ii) the magnitude of the mean squared displacement. However, while both the potential energy and final values of MSD exhibit trends towards an equilibrium value for each simulation, they do not exhibit an overall trend towards an absolute value representing a homogeneous glass. Glass A1, for example, has a higher potential energy, Figure 1, than both glass A2 and class B, despite having a significantly longer equilibration period. Similarly, glass C, which is the result of an immediate quench, would be expected to have one of the highest PEs. It, however, has a value lying between glasses D4 (equilibrated at 3500 K) and D5 (equilibrated at 4500 K). The final value of MSD for glass E, which was

completely simulated at 300 K, would be expected to be the highest as its structure most closely resembles the initial starting configuration. However, glass C has the highest final MSD value with glass E lying close to class D and glass A1. Therefore, glass E's ionic diffusion is being *hindered* rather than assisted by its high potential energy. Hence, for these simulations, the inter-relationship between potential energy, MSD and configuration is not entirely obvious or straightforward and their value in indicating the degree of homogeneity is therefore questionable.

The structure, e.g. RDFs, could also only be used as an indicator of equilibration rather than homogeneity since the structure tends to a configuration dictated by both the potential and the simulation methodology. In addition, this study has shown that a single structural analysis technique may not give an accurate picture of the structural trends. For example, although the RDF peak heights, in general, decrease (Fig. 6) as the equilibration and simulation period increases, the Zr–F RDF first peak height does not. Neither are any significant changes observed in the average coordination numbers and NNADs for Zr–F, Table IV and Figure 7. However, the Zr–F CND for glass E, Figure 7, is significantly different in both width and average coordination number from those produced by glasses A1, B1 and C.

A comparison of the ionic spherical averages, n_{all} to n^*_{all} and of n_j to n^*_j (Figs. 4 and 5), provided a much better insight into the homogeneity of the liquid than either the potential energy, final MSD value or structural results. They also provided a guide for the equilibration process. In these figures, the spherical average of all ions in the system, n_{all}, and the spherical average of ions of the same type, n_j, are plotted. As the simulated structure becomes more homogeneous, the values of n_{all} and n_j approach those for a homogeneous glass. The rate of approach gives an indication as to how fast the simulation is approaching equilibrium. Monitoring equilibrium and homogeneity during the complete simulation was therefore possible. The value of n_j was particularly useful as it indicated the particular ion type(s) that were not homogeneously mixed. For example, Figure 5 indicates that while the fluorine ions, due to their higher mobility and zirconium ions, due to their higher charge, are fully equilibrated in glass C, barium only reaches equilibrium in glass A1.

Selecting a particular temperature for a molecular dynamics simulation relies on changing the particle velocity, i.e. controlling the energy of the system by connecting it to a heat bath. Hence, the simulation temperature was set using the NVT ensemble. Moving from the NVT ensemble to the NVE ensemble in glass simulations A1 and A2 resulted in a decrease in

potential energy with a corresponding increase in temperature (observable in the temperature shift for glass A1 in the inset graph on Fig. 1). Thus, the NVT ensemble simulation may not allow complete structural relaxation. Hence, a combination of constant NVT and NVE conditions were used rather than simply constant NVT. The optimum ensemble for data collection is therefore the NVE ensemble. A further advantage using the NVE ensemble for data collection is that as the system is not being perturbed by energy in flow and out flow. The greatest reduction in n_{all} within the first 20 ps occurred for the class A glasses, i.e. those simulated using both constant NVT and NVE conditions. Therefore, the combination of constant NVE and NVT conditions also led to a more rapid equilibration than simply constant NVT.

The equilibration temperature and the equilibration ensemble are equally important, Figure 3. as too low a temperature causes inadequate diffusion leading to either an unequilibrated structure or a prohibitively long equilibration period. Similarly, if the equilibration temperature is too high, the quench rate will either be too high or the quench period lengthy, e.g. glass B2. As in experiment, the equilibration temperature should be in the liquid region where diffusion is rapid, i.e. above the glass transition temperature, T_g. The change in slope of the PE versus temperature curve, as well as the final MSD curve, indicated that the effective glass transition region was at approximately 2000 K in these simulations, Figures 1 and 2. This is consistent with earlier simulations [33]. The consequence of the effective glass transition region on equilibration is shown by a sharp increase in the values of n_{all} between 3000 K and 2500 K for the isothermal simulations. This corresponded to a sharp decrease in homogeneity, Figure 3. An abrupt decrease in the average coordination numbers for Ba–Ba, Na–Na and Zr–Zr above 3000 K is also observed, Table IV. Therefore, to ensure a reasonably short equilibration period, the optimum equilibration temperature is one which is well above the effective simulation glass transition temperature. However, a comparison of the n_{all} values for glasses B2 and B3 shows that a very high equilibration temperature does not necessarily result in a more homogeneous structure. A equilibration temperature of 3 times the effective glass transition temperature (6000 K) was found most suitable. The effective simulation glass transition temperature is, of course, dependent on the time scale of the quench as well as the simulation parameters (potential, constant volume or constant pressure, etc).

The equilibration period was chosen carefully as it had a dramatic effect on the final structure. As stated earlier both the PE and final MSD curves only provided a guide to the degree of equilibration and not homogeneity.

Therefore, high temperature equilibration was only considered complete when the values of n_{all} and n_j had stabilised and approached their homogeneous values. This approach to equilibrium was, as expected, of an exponential nature (shown by the inset graph in Fig.3) with a very long time constant despite the high diffusion rates, Figure 2. This exponential nature of equilibration was also shown by the minor structural differences between glass A1 and, glass A2, glass C and class B despite the significant variation in equilibration period. The structure of one the slowest moving ions, Ba, was the most effected by insufficient initial equilibration (Zr, the other slow moving ion, was not effected due to its higher charge). The splitting of the Ba–Ba RDF peak in glass A1, when compared with glass A2 and class B, was solely a result of the increased equilibration period. Starting from an inhomogeneous structure, an equilibration period that enabled barium to move, on average, a distance equivalent to 3 times the box length was required.

Insufficient diffusion during the quenching process may result in insufficient structural relaxation. This causes n_{all} to deviate from that of a homogeneous distribution and clustering to result. A comparison of n_{all} for glasses B3 and C, which share the same high temperature melt, shows this behaviour, Figure 3. Glass C is the result of an immediate quench from 6000 K to 300 K, whereas glass B3 had a significantly slower quench rate, see Table II. Despite some structural relaxation due to its initially very high potential energy, the value of n_{all} for glass C is still much greater than that for glass B3 at 300 K. Similarly, the values of n_{all} vary more for glass A2 when compared with glass A1 which had a slower quench rate. Therefore, the ideal quench rate is one which is sufficiently slow so as to keep the fluctuations in n_{all} to a minimum.

Although, in general, the structural accuracy decreases as the equilibration periods and quench rate decrease, some surprising contradictions do occur. Glass, C, produced by an immediate quench, has RDFs that are very similar to those of the much longer simulation, glass A2. However, the NNADs and CNDs not containing Zr are different. Therefore, glass C can be used to give broad structural accuracy during the potential function tuning process when simulation time is of primary importance. Glass A2 approaches the structure of glass A1, the major differences being in the RDFs of Ba–Ba and Ba–Na, and can be used for a more accurate structural comparison. However, the longest simulation, glass A1 gave the most accurate and realistic results and is the optimum for final verification of the potential as well as all data collection.

CONCLUSION

This study has shown that the simulation methodology is at least as important as the potential in determining the final glass structure. The melt equilibration period, quench rate and simulation ensembles all had an effect on the structure. This was highlighted by differences between the structures of glass A1, B1 and glass E.

Two useful tools, a spherical average of all ions in the system, n_{all}, and the spherical average of each ion type, n_j, have been developed which can, with more accuracy than present techniques, indicate the degree of homogeneity or equilibration in glass simulation. Ions types that are not homogeneously distributed could also be identified.

Various simulation strategies can be used during the potential tuning process depending on the structural accuracy required. During the initial tuning process a short simulation utilising an immediate quench can be used, as in glass C. This simulation gave a broad agreement in the radial distribution functions with that of the most equilibrated glass, glass A1. The method of glass A2 can be used during the latter stages of the tuning process when a better agreement with glass A1 was desired. However, the best agreement with experimental values was only obtained by the simulation methodology of glass A1. Thus, the simulation methodology and hence, simulation time, can be varied so as to give the desired structural accuracy.

The use of canonical ensemble (NVT) for a constant volume simulation led to a structure which was not in its minimum potential energy configuration. A combination of the canonical (NVT) and microcanonical (NVE) ensembles was therefore used to provide the lowest potential energy configuration. As a result, data collection was only performed during the NVE ensemble. The NVE ensemble has an added benefit for data collection in that the system is not being perturbed by energy in flow and out flow.

Finally, the methodology of glass A1 appears optimal for molecular dynamics simulations of the type performed in this paper.

References

[1] France, P. W., Drexhage, M. G., Parker, J. M., Moore, M. W., Carter, S. F. and Wright, J. V. (1992). *Fluoride Glass Optical Fibres*, Blackie, Glasgow and London.

[2] Wright, A. C. (1993). "Neutron and X-ray Amorphography," in *Experimental Techniques of Glass Science*, Simmons, C. J. and El-Bayoumi, O. H., Eds. Westerville: American Ceramic Society, pp. 205–314.

[3] Angell, C. A., Cheesemann, P. A. and Tamaddon, S. (1982). "Computer Simulation studies of migration mechanisms in ionic glasses and liquids", *Journal de Physique* C9, **43**, 291–301.
[4] Lucas, J., Angell, C. A. and Tamaddon, S. (1984). "Fluoride bridging modes in fluorozirconate glasses by X-ray and computer simulation studies", *Mat. Res. Bull.*, **19**, 945–951.
[5] Yasui, I. and Inoue, H. (1985). "Molecular dynamic simulations of changes in structure in ZrF4 based glasses", *J. Non-cryst. Solids*, **71**, 39–47.
[6] Kawamoto, Y., Horisaka, T., Hirao, K. and Soga, N. (1985). "A molecular dynamics study of barium meta-fluorizirconate glass", *J. Chem. Phys.*, **83**, 2398–2404.
[7] Phifer, C. C. and Lucas, J. (1987). "A new perspective on fluorozirconate glass structure", *Mat. Sci. Forum*, **19–20**, 111–120.
[8] Wright, A. C. (1993). "The comparison of molecular dynamics simulations with diffraction experiments", *J. of non-cryst. solids*, **159**, 264–268.
[9] Hamill, L. T. and Parker, J. M. (1985). "Hydrogen Solubility in heavy metal fluoride glasses", *Phys. Chem. Glasses*, **26**, 52–54.
[10] Simmons, J. H., Faith, R. and O'Rear, G. (1987). "Molecular Dynamic Simulations of fluoride glass structures", *Mat. Sci. Forum*, **19–20**, 121–126.
[11] Phifer, C. C., Angell, C. A., Laval, J. P. and Lucas, J. (1987). "A Structural Model for Prototypical Fluorozirconate Glass", *J. Non-cryst. Solids*, **94**, 315–335.
[12] MacFarlane, D. R., Inoue, S., Browne, J. O. and Uhlherr, A. (1988). "Prediction of Glass Formation in Heavy Metal Fluoride Systems by molecular dynamics simulation", *Mat. Sci. Forum*, **32–33**, 125–130.
[13] Boulard, B., Kieffer, J., Phifer, C. C. and Angell, C. A. (1992). "Vibrational spectra in Fluoride Crystals and Glasses at normal and high pressures by computer simulation", *J. Non-cryst. Solids*, **140**, 350–358.
[14] Brawer, S. A. and Weber, M. J. (1981). "Molecular dynamics simulations of the structure of rare-earth-doped beryllium fluoride glasses", *J. Chem. Phys.*, **75**, 3522–3541.
[15] Hockney, R. W. and Eastwood, J. W. (1994). *Computer Simulation using Particles*, Adam Hilger, London.
[16] Amini, M., Eastwood, J. W. and Hockney, R. W. (1987). "Time integration in particle models", *Comp. Phys. Comms.*, **44**, 83–93.
[17] Allen, M. P. and Tildesley, D. J. (1990). *Computer Simulation of Liquids*, Oxford University Press.
[18] Amini, M. and Fincham, D. (1990). "Evaluation of temperature in molecular dynamics simulations", *Comp. Phys. Comms.*, **56**, 313–324.
[19] Rahman, A., Fowler, R. H. and Narten, A. H. (1972). "Structure and motion in liquid BeF_2, $LiBeF_3$, and LiF from molecular dynamics calculations", *J. Chem. Phys.*, **57**, 3010–3011.
[20] Gruenhut, S. and MacFarlane, D. R. (1995). "Molecular dynamics simulation of heavy metal glasses: comparison of Buckingham and BHM potentials", *J. Non-cryst. Solids*, **184**, 356–362.
[21] Laval, J. P. and Abaouz, A. (1992). "Crystal Structure of $BaNaNr_2F_{11}$: A Phase Recrystallizing from Fluorozirconate Glasses", *J. of Solid State Chem.*, **101**, 18–25.
[22] Dunitz, J. D. (1979). *X-ray analysis and the structure of organic molecules*, Cornell University Press, New York.
[23] Walker, J. R. (1982). "Molecular dynamics simulations of crystalline ionic materials", in *Computer Simulations of Solids*, eds. Catlow, C. R. A. and Mackrodt, W. C., Springer-Verlag, Berlin, ch.5.
[24] *Catalysis User Guide 2.3.0*, Biosym Technologies, San Diego, USA (1993).
[25] McQuarrie, D. A. (1976). "Statistical Mechanics", Harper Collins Publishers Inc., New York.
[26] Almeida, R. M. and Mackenzie, J. D. (1981). "Vibrational spectra and structure of fluorizirconate glasses", *J. Chem. Phys.*, **74**, 5954–5961.
[27] Coupe, R., Louer, D., Lucas, J. and Leonard, A. J. (1983). "X-Ray scattering studies of glasses in the system ZrF_4-BaF_2", *J. of. Am. Ceramics Soc.*, **66**, 523 529.
[28] Ko, S.-H. and Doremus, R. H. (1991). "Infrared spectra and structure of fluorozirconate glasses", *Phys. Chem. Glasses*, **32**, 196–201.

[29] Wagner, C. N. J., Jost, S. B., Etherington, G., Boldrick, M. S., Almeida, R. M., Faber, J. J. and Volin, K. (1987). "The structure of heavy metal fluoride glasses", *Mat. Sci. Forum.*, **19–20**, 137–140.

[30] Kawamoto, Y. and Horisaka, T. (1983). "Short-range structures of barium, lead and strontium meta-fluorozirconate glasses", *J. Non-cryst. Solids*, **56**, 39–44.

[31] Uhlherr, A., MacFarlane, D. R., Moore, L. J. and Thomas, P. D. (1991). "Molecular Dynamics investigation of the Structure and Stability of zirconium-barium-rare earth fluoride glasses", *Mat. Sci. Forum*, **67 & 68**, 431–436.

[32] Wang, W. C., Chen, Y. and Hu, T. D. (1993). "Effect of Alkali Fluoride on the short range structures of ZrF_4-BaF_2 based glasses", *Phys. Stat. Sol. (A)*, **136**, 301–310.

[33] Angell, C. A., Clarke, J. H. R. and Woodcock, V. (1981). "Interaction Potentials and Glass Formation: A survey of computer experiments", in *Advances in Chemical Physics*, eds. Prigogine, I. and Rice, S. A., **48**, 397.